

# Rotational dynamics of proteins from spin relaxation rates and molecular dynamics simulations

O. H. Samuli Ollila\*

*Institute of Biotechnology, University of Helsinki*

(Dated: May 10, 2017)

## I. INTRODUCTION

Spin relaxation rates measured with NMR techniques give segmental resolution information about rotational dynamics of proteins and macromolecules. Various models have been used to separate internal dynamics and order from overall rotational diffusion of molecules [? ]. These techniques have been highly useful in characterization of rotational diffusion and internal flexibility of proteins and other biomolecules. On the other hand, segmental level information has been used in validation and improvement of molecular dynamics simulation force fields [? ]. Segmental order has been also related to conformational entropy of proteins [? ].

Spin relaxation rates are typically interpreted by using various dynamical models assuming different level of complexity of rotational relaxation processes. The most simplistic models assume single timescale and order parameter for internal motion and isotropic overall rotational diffusion. However, biomolecules often experience anisotropic overall diffusion and several internal timescales. Models for more complicated models have been also introduced, however, there are more fitting parameters in these models and interpretation of experiments becomes extensively difficult.

Classical molecular dynamics simulations contain, in principle, all the complexity of the timescales and could be used to interpret the rotational dynamics measured with spin relaxation experiments. However, this has not been a trivial task due to the force field issues and limited available time scales in the simulations.

In this work we present approach that can be used to analyze spin relaxation experiments by using classical molecular dynamics simulations. The approach can be used for anisotropic molecules and allows a correction of anisotropic overall diffusion. We demonstrate the usage of the approach for two anisotropic protein constructs from engineered from *Helicobacter pylori* and *Pseudomonas*.

## II. METHODS

### A. Spin relaxation and rotational dynamics of molecules

Spin relaxation rates  $R_1$ ,  $R_2$  and  $R_{\text{NOE}}$  measured from NMR experiments for N-H bonds are related to the molecular

dynamics through spectral density  $J(\omega)$  and equations [1, 2]

$$R_1 = \frac{d_{\text{NH}}^2 N_{\text{H}}}{20} \left[ J(\omega_{\text{H}} - \omega_{\text{N}}) + 3J(\omega_{\text{N}}) + 6J(\omega_{\text{N}} + \omega_{\text{H}}) \right] + \frac{(\sigma\omega_{\text{N}})^2}{15} j(\omega_{\text{N}}), \quad (1)$$

$$R_2 = \frac{1}{2} \frac{d_{\text{NH}}^2 N_{\text{H}}}{20} \left[ 4J(0) + 3j(\omega_{\text{N}}) + J(\omega_{\text{H}} - \omega_{\text{N}}) + 6J(\omega_{\text{H}}) + 6J(\omega_{\text{N}} + \omega_{\text{H}}) \right] + \frac{(\sigma\omega_{\text{N}})^2}{15 \cdot 6} [4J(0) + 3J(\omega_{\text{N}})], \quad (2)$$

$$R_{\text{NOE}} = 1 + \frac{d_{\text{NH}}^2 N_{\text{H}}}{20} \left[ 6J(\omega_{\text{N}} + \omega_{\text{H}}) + J(\omega_{\text{H}} - \omega_{\text{N}}) \right] \frac{\gamma_{\text{H}}}{\gamma_{\text{N}} R_1}, \quad (3)$$

where  $\omega_{\text{N}}$  and  $\omega_{\text{H}}$  are the Larmor angular frequencies of  $^{15}\text{N}$  and  $^1\text{H}$  respectively,  $N_{\text{H}}$  is the number of bound protons. The dipolar coupling constant is given by

$$d_{\text{NH}} = -\frac{\mu_0 \hbar \gamma_{\text{H}} \gamma_{\text{N}}}{4\pi \langle r_{\text{CN}}^3 \rangle},$$

where  $\mu_0$  is the magnetic constant or vacuum permeability,  $\hbar$  is the reduced Planck constant,  $\gamma_{\text{N}}$  and  $\gamma_{\text{H}}$  are the gyro-magnetic constants of  $^{15}\text{N}$  and  $^1\text{H}$ , respectively. Average cubic length is  $\langle r_{\text{CN}}^3 \rangle \approx$  and the chemical shift anisotropy is  $\Delta\sigma \approx 160 \cdot 10^{-6}$  for N-H bonds in proteins [? ].

Spectral density  $J(\omega)$  is the Fourier transformation of the second order rotational correlation function for N-H bond

$$J(\omega) = 2 \int_0^\infty C(t) \cos(\omega t) dt. \quad (4)$$

The second order rotational correlation is defined as

$$C(t) = \langle (3 \cos^2 \theta_{t'; t'+t} - 1) / 2 \rangle_{t'}, \quad (5)$$

where average is ensemble average and  $\theta$  is the angle between N-H bonds at times  $t'$  and  $t' + t$ . The rotational correlation function for protein tumbling in solution contains information about overall rotation of the molecule as well as internal relaxation processes. Assuming that these are independent, the rotational correlation function can be written as [? ]

$$C(t) = C_I(t) C_O(t), \quad (6)$$

where  $C_I(t)$  and  $C_O(t)$  are correlation functions for internal and overall rotations, respectively. Correlation function for fully anisotropic overall rotation can be written as a sum of

\* samuli.ollila@helsinki.fi; Department of Neuroscience and Biomedical Engineering, Aalto University

five exponentials [? ]

$$C_O(t) = \sum_{j=1}^5 A_j e^{-t/\tau_j}, \quad (7)$$

where time constants  $\tau_j$  are related [3] to the diffusion constants around three principal axes of a molecule  $D_{xx}$ ,  $D_{yy}$  and  $D_{zz}$ , defined as

$$\begin{aligned} \langle (\Delta\alpha_{t';t'+t})^2 \rangle_{t'} &= 2D_{xx}t \\ \langle (\Delta\beta_{t';t'+t})^2 \rangle_{t'} &= 2D_{yy}t \\ \langle (\Delta\gamma_{t';t'+t})^2 \rangle_{t'} &= 2D_{zz}t, \end{aligned} \quad (8)$$

where  $\langle (\Delta\alpha_{t';t'+t})^2 \rangle_{t'}$ ,  $\langle (\Delta\beta_{t';t'+t})^2 \rangle_{t'}$  and  $\langle (\Delta\gamma_{t';t'+t})^2 \rangle_{t'}$  are mean square angle deviations of protein inertia axes. The internal correlation function decays to a plateau, which defines the square of order parameter respect to molecular axes  $S^2$ . The effective internal correlation time can be defined with the help of reduced correlation function  $C'_I(t) = (C_I - S^2)/(1 - S^2)$  [? ]

$$\tau_{\text{eff}} = \int_0^\infty C'_I(t) dt. \quad (9)$$

Standard analyses of experimental relaxation data usually assume fully or axially isotropic overall rotational motion and single decay constant for internal motion. Then the free parameters ( $S^2$ ,  $\tau_j$ ,  $A_j$ ) are fit against spin relaxation data from experiments. This gives most likely very good results for isotropic molecules for which the assumption of single internal motional timescale is reasonable. However, for molecules with significant shape anisotropy or several timescales in internal motions the amount of parameters to be fitted becomes large compared with the typical amount of experimental points.

## B. Rotational dynamics from molecular dynamics simulations

Classical molecular dynamics simulations give trajectories of individual atoms as a function of time, which can be used to calculate rotational correlation functions for each bond and explicit separation of internal and overall rotational motions of molecules. The rotational correlation functions can be used to calculate spin relaxation times through Eqs. 1-4, which can be then compared to the experimental data in order to assess simulation model quality [? ] and interpret experiments [? ]. However, the comparison is often complicated by the short simulation times [? ] and incorrect overall rotational diffusion due to water models [? ]. These issues have been typically overcome by introducing isotropic rotational diffusion term in the correlation functions [? ] or comparing order parameters instead of spin relaxation rates [? ]. These approaches are not, however, useful for anisotropic proteins and order parameter comparison is not direct comparison between simulations and experiments in the case of freely rotating molecules.

Method presented here can be applied also to anisotropic

proteins simulated with timescales routinely accessible with state of the art computational infrastructure. The key idea of the method is to calculate the rotational diffusion constants and then use Eq. 7 to determine the correlation function related to the overall rotational diffusion.

Here we present method to analyse rotational dynamics. The analysis of rotational dynamics performed in this work can be divided in essentially six steps listed here.

- 1) Total rotational correlation functions  $C(t)$  for protein N-H bonds are calculated from MD simulation trajectory by applying Eq. 5.
- 2) Rotational correlation functions for internal dynamics  $C_I(t)$  are calculated from a trajectory from where the overall rotation of protein is removed.
- 3) The overall and internal motions are assumed to be independent and overall rotational correlation function is calculated as  $C_O(t) = C(t)/C_I(t)$  according to Eq. 6.
- 4) The protein axes of inertia and their mean square deviations as function of time are calculated from MD simulation trajectory.
- 5) Rotational diffusion constants  $D_x$ ,  $D_y$  and  $D_z$  are calculated by fitting a straight line to mean square angle deviations of inertia axes according to Eq. 8.
- 6) Timescales in Eq. 7 are calculated from diffusion constants and weighting factors  $A_j$  are determined by fitting the equation to rotational correlation functions of overall rotational motion  $C_O(t)$  determined in step 3).
- 7) New total rotational correlation functions  $C_N(t)$  are determined by multiplying internal correlation function  $C_I(t)$  from step 2) by Eq. 7 with parameters from step 6). Rotational diffusion constants (and  $\tau_i$  values in Eq. 7) can be also divided by a scaling factor at this point to tune overall rotational diffusion in rotational dynamics model close to experimental value.

## C. Simulation and analysis details

Simulations were ran using Gromacs 5 [4] And Amber ff99SB-ILDN [5] force field for proteins. The proteins were solvated to tip3p[6], tip4p [6] or OPC4 [7] water models. NMR structures from [? ] and [8] are used as initial structure for PaTonB and HpTonB-92, respectively. Temperature was coupled to desired value with v-rescale thermostat [9] and pressure was isotropically set to 1 bar using Parrinello-Rahman barostat [10]. Timestep was 2 fs, Lennart-Jones interactions were cut-off at 1.0 nm, PME [11, 12] was used for electrostatics and LINCS was used to constraint all bond lengths [13]. Simulation trajectory and related files are available at [??]. The simulated systems are listed in Table I

The rotation is removed by using fit option in *gmx trjconv* and rotational correlation functions are calculated with *gmx rotacf* [14]. Inertia axes of protein are calculated with *compute\_inertia\_tensor* from MDTraj python library [15]. The spectral density was calculated by first fitting the sum of 471 exponentials having correlation times from 1 ps and 50 ns with

logarithmic spacing to the new correlation function

$$C_N(t) = \sum_{i=1}^N \alpha_i e^{-t/\tau_i}, \quad (10)$$

by using the *lsqnonneg* routine in MATLAB [16]. The Fourier transform is then calculated by using analytical function for the sum of exponentials

$$J(\omega) = 4 \sum_{i=1}^N \alpha_i \frac{\tau_i}{1 + \omega^2 \tau_i^2}. \quad (11)$$

Similar approach is used previously for lamellar systems in combination with solid state NMR experiments [17, 18].

### III. RESULTS AND DISCUSSION

#### A. Global rotational dynamics of protein

Mean square angle deviations of protein inertia axes as a function of time from PsTonB simulations are shown in Fig. 1. Diffusion coefficients are calculated from linear fits by taking into account lag times less than hundredth of the total simulation length, which is expected to give good statistics for rotation of single molecules in MD simulations [? ]. Linear diffusion fit to mean square angle displacement seems fairly good in Fig. 1, however, log-log plot shown in 7 reveals some anomalous diffusion behaviour at time scales below 0.12 ns. Here we use diffusion coefficients to include protein overall motion in spin relaxation calculations and the effect of small anomaly with short timescales is beyond the scope of the work.

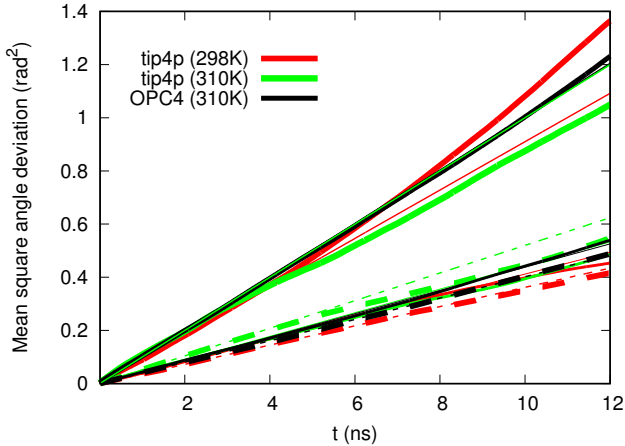


FIG. 1. The inertia tensor angles as a function of time and mean square angular deviations for PsTonB simulation with OPC water model.

The results for diffusion constants from different simulations shown in Table I are in line with previous results from experiments [? ] and simulations [? ] for more isotropic

proteins. As expected, rotational diffusion is faster in simulations with higher temperature or smaller protein. Also the larger diffusion constants for simulations with tip3p are expected due to the low viscosity of the model [? ].

Inclusion of rotational diffusion coefficients in N-H bond rotational correlation functions is exemplified in Fig. 2 for residue 331 located in alpha helix of PaTonB protein. The same analysis is performed also to other bonds and the resulting correlation functions are used to calculate spin relaxation rates. As expected, the N-H bond correlation functions calculated from original MD trajectories shown in Fig. 2 A) decay to fluctuate approximately around zero after  $\sim 20$  ns. Fluctuations from ideal relaxation behaviour begin already close to one hundredth of total simulation time (approximately 4-12 ns for the studied systems), which is expected to be the limit for good statistic for rotational dynamics analyzed from single molecule MD simulation [? ]. Internal correlation functions, calculated from trajectory with overall protein rotation removed, in Fig. 2 B) show rapid decay to a plateau value, which defines the square of the order parameter  $S^2$ . The global rotational correlation functions calculated as  $C_O(t) = C(t)/C_I(t)$  are shown in Fig. 2 C).

Overall rotational correlation functions were fit to Eq. 7, where timescales for anisotropic rotation [3] were determined by using rotational diffusion constants from Table I, to determine the prefactors  $A_j$  for all residues. Result for such fit are exemplified with dashed lines in Fig. 2 C) for residue 331 of PsTonB. The prefactors, global rotational timescales and correlation functions for internal relaxation were used to determine new correlation function  $C_N(t) = C_I(t) \sum_{j=1}^5 A_j e^{-t/\tau_j}$ , where internal correlation comes directly from MD simulation and global rotational correlation function from diffusion coefficients calculated from MD and Eq. 7. The new correlation functions are exemplified with dashed lines in Fig. 2 A) for residue 331 of PsTonB.

#### B. Global rotational dynamics in simulations and experiments

Spin relaxation rates were calculated from MD simulations by using new correlation functions, where global rotational dynamics is described by Eq. 7 with timescales from diffusion constants in Table I and prefactors fit to the MD simulation data. The results for PaTonB and HpTonB simulations with different water models are shown in Figs. 3 and ??, respectively.

For PaTonB  $T_1$  and  $T_1/T_2$  ratio are slightly underestimated systemically in all simulations. For HpTonB tip4p gives good agreement with experiments but tip3p results are significantly off. Underestimation of  $T_1/T_2$  ratio suggests that the global rotational diffusion is overestimated in simulations [? ]. Thus, we tested if scaling of diffusion coefficients with constant factor gives better agreement with experiments. Rotational diffusion coefficients for PaTonB simulation with tip4p and HpTonB simulation with tip3p were first divided by factors 1.2 and 2.9, respectively. Then, the new correlation functions  $C_N(t)$  were calculated by using timescales determined from scaled diffusion constants and prefactors from the fit to

TABLE I. Simulated systems and rotational diffusion coefficients ( $\text{rad}^2 \cdot 10^7/\text{s}$ ) calculated from simulations.

Protein	Water model	T (K)	$t_{\text{sim}}$ (ns)	$t_{\text{anal}}$ (ns)	$D_{xx}$	$D_{yy}$	$D_{zz}$	$D_{  }/D_{\perp}$	$D_{av}$	files
PaTonB	tip4p	298	400	390	$1.81 \pm 0.01$	$2.06 \pm 0.03$	$4.55 \pm 0.03$	$2.35 \pm 0.04$	$2.80 \pm 0.02$	[?]
PaTonB	tip4p	310	400	390	$2.60 \pm 0.02$	$2.22 \pm 0.05$	$5.0 \pm 0.1$	$2.07 \pm 0.09$	$3.26 \pm 0.07$	[?]
PaTonB	OPC4	310	1200	1190	$2.01 \pm 0.01$	$2.19 \pm 0.01$	$5.01 \pm 0.03$	$2.39 \pm 0.02$	$3.07 \pm 0.01$	[?]
HpTonB-92	tip3p	310	570	370	$8.25 \pm 0.05$	$7.67 \pm 0.06$	$15.9 \pm 0.3$	$1.99 \pm 0.06$	$10.6 \pm 0.2$	[?]
HpTonB-92	tip3p	303	800	790	$6.24 \pm 0.02$	$7.04 \pm 0.03$	$11.9 \pm 0.2$	$1.80 \pm 0.03$	$8.40 \pm 0.07$	[?]
HpTonB-92	tip4p	310	470	370	$3.6 \pm 0.1$	$3.24 \pm 0.01$	$6.3 \pm 0.3$	$1.8 \pm 0.1$	$4.4 \pm 0.2$	[?]
HpTonB-92	tip4p	303	400	200	$2.7 \pm 0.1$	$2.71 \pm 0.02$	$5.6 \pm 0.5$	$2.1 \pm 0.2$	$3.7 \pm 0.2$	[?]
HpTonB-92	OPC4	310	800	790	$2.85 \pm 0.01$	$2.70 \pm 0.01$	$5.56 \pm 0.01$	$2.00 \pm 0.01$	$3.70 \pm 0.01$	[?]

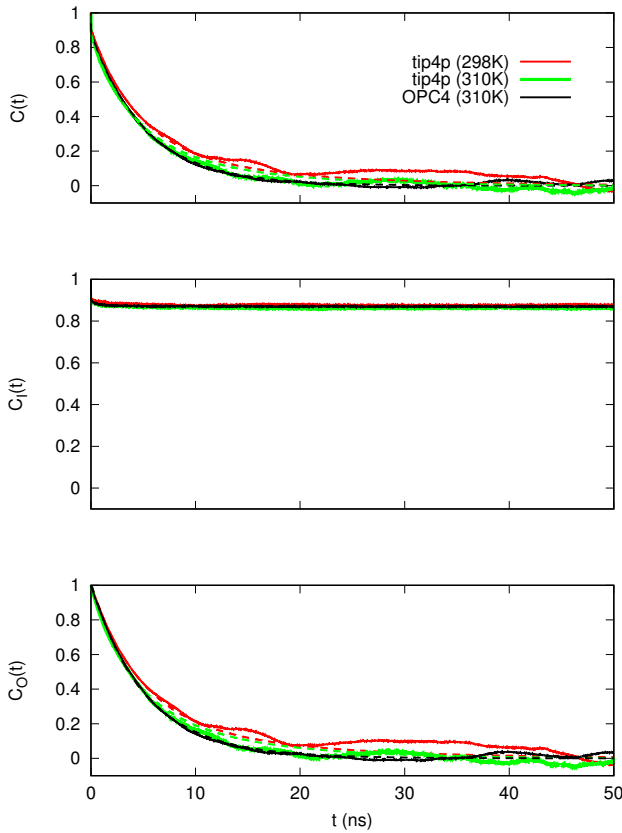


FIG. 2. Example correlation functions for residue 331 of PsTonB calculated from MD simulations with different water models. A) total correlation functions  $C(t)$  calculated from MD simulation (solid lines) and new correlation functions determined from Eqs. 6 and 7 by using rotational diffusion constants and fitted prefactors (see section II B) (dashed lines), B) correlation function for internal motions and C) correlation function for overall motions determined from Eq. 6 ( $C_O(t) = C(t)/C_I(t)$ ) (solid lines) and fits to Eq. 7.

the overall correlation functions. The spin relaxation results from these correlation functions are shown in Figs. 5 and 6 for PsTonB and HpTonB, respectively, are in good agreement with experiments. This suggests that the new correlation func-

tions with the scaled diffusion coefficients can be used to interpret the protein rotational dynamics from NMR relaxation data.

The rotational diffusion coefficients after the scaling are shown in Table II. These diffusion constants applied in the global rotational correlation functions give spin relaxation times in good agreement with experiments, thus these can be considered as an interpretation of NMR relaxation data. The diffusion coefficients from tip3p simulation for HpTonB-92 with scaled diffusion constants (Table II) and slightly smaller than diffusion coefficients from tip4p simulation (Table I), which also gave a relatively good agreement with experiments. However, the scaled results from tip3p simulation gives slightly better agreement for  $T_1/T_2$  ratio and, thus, a better interpretation for experiments.

TABLE II. Rotational diffusion coefficients scaled with constant factor which gives a good agreement for spin relaxation data, 2.9 for tip3p simulation of HpTonB and by 1.2 for tip4p simulation of PsTonB.

	HpTonB-92	PsTonB
$D_{xx}$	$2.15 \pm 0.01$	$1.51 \pm 0.01$
$D_{yy}$	$2.43 \pm 0.01$	$1.72 \pm 0.03$
$D_{zz}$	$4.10 \pm 0.01$	$3.79 \pm 0.03$
$D_{av}$	$2.90 \pm 0.03$	$2.3 \pm 0.02$
$\tau_c(\text{ns})$	$5.7 \pm 0.1$	$7.2 \pm 0.1$

### C. Protein internal relaxation

Simulations in good agreement with spin relaxation data can be used to interpret internal relaxation and order of proteins. For example, in PsTonB low order parameters and larger effective correlation times are observed in Fig. 3 B) for residues 246-251 in N-terminus, residues 260-274, residues 300-303, residues 320-326 and residues 338-342 in C-terminus. The results in terminal ends (residues 246-251 and 338-342) can be explained by the increased flexibility of unstructured endings of the protein, which are also seen in overlaid structures in Fig. 3 A). Low order parameters and large effective correlation times between residues 260-274 arise from two different orientations sampled by alpha

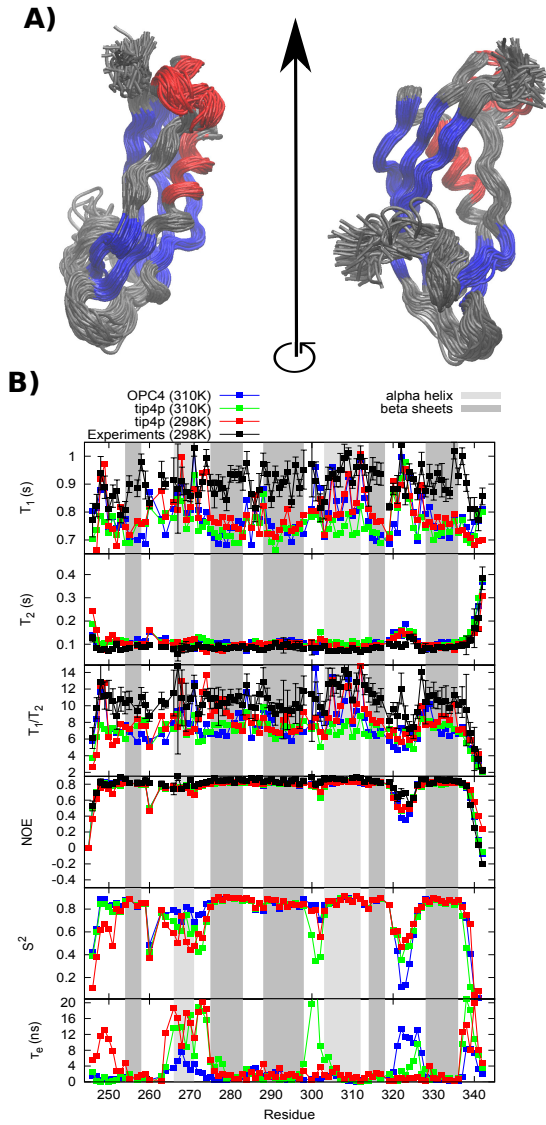


FIG. 3. A) Structures sampled by PsTonB from MD simulations (100 structures from 400ns long trajectory). B) Spin relaxation rates, order parameters and effective internal correlation times from experiments and simulations. Spin relaxation rates indicate increased flexibility only for the last two residues in N terminus. However, MD simulations suggest somewhat smaller order parameters and longer  $\tau_e$  for residues 246-253. By looking at the sampled structures, it seems that lower order parameters and longer correlation times arise from slower and less extensive conformational sampling than in HpTonB-107. Lower order parameters and larger correlation times are also observed in PsTonB simulations between residues 265-275. This can be explained by the changes in orientation of alpha helix close to this region, as seen in the sampled conformations. Such effect was not seen in the HpTonB simulations, however, NMR data for this region showed some unclarities which may arise from such conformational exchange. Enhanced sampling is also observed between residues 320-326. This was not observed in HpTonB samples, which may be related to the formation of beta sheet between residues 315-318 in PsTonB. Relaxation parameters for PsTonB from experiments and simulations with Amber-ildn and different water models

helix on that region, as also seen in Fig. 3 A). This explains

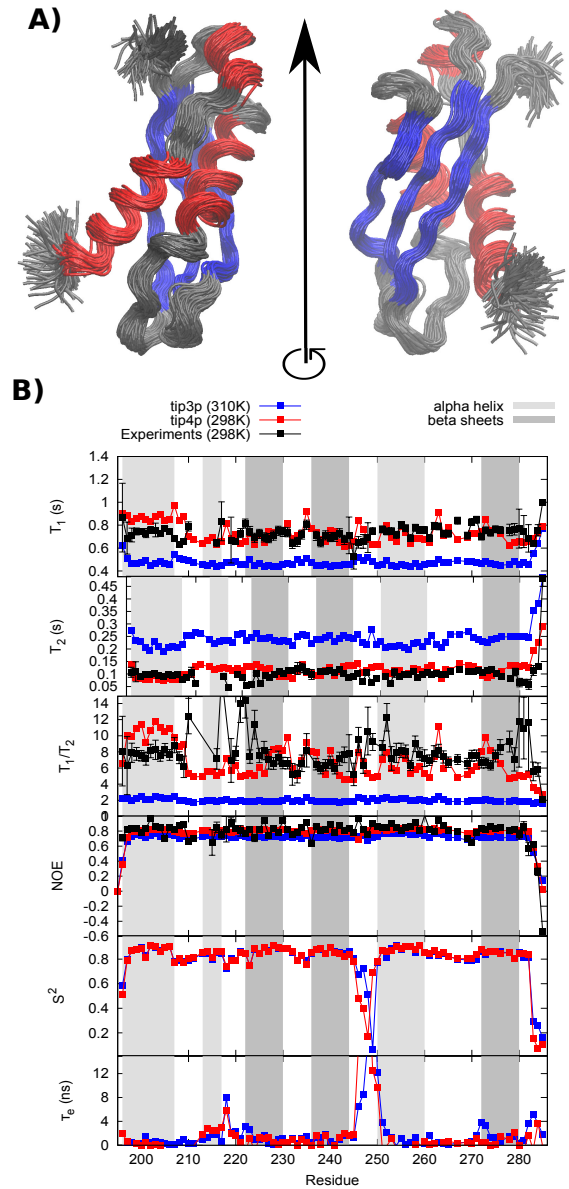


FIG. 4. Relaxation parameters for HpTonB short construct from experiments and simulations with Amber-ildn and different water models

also the lower resolution in NMR spectra observed for that region [? ]. Between residues 320-326 decrease in NOE and  $T_1/T_2$  ratio and increase in  $T_2$  are also observed in simulations and experiments. The results can be explained by the increased flexibility of the loop in this region as also seen in overlayed structures. Low order parameters and large effective correlation times between residues 300-303 are not seen in spin relaxation data, thus it is not clear if these arise from simulation artefact.

Also for HpTonB low order parameters and long effective correlation times are observed only for flexible terminal ends (residues 196-197 and 283-285) as seen in Fig. ?? . Low order parameters and long effective correlation times and for residues 245-250 probably arise (at least partly) from simulation arte-

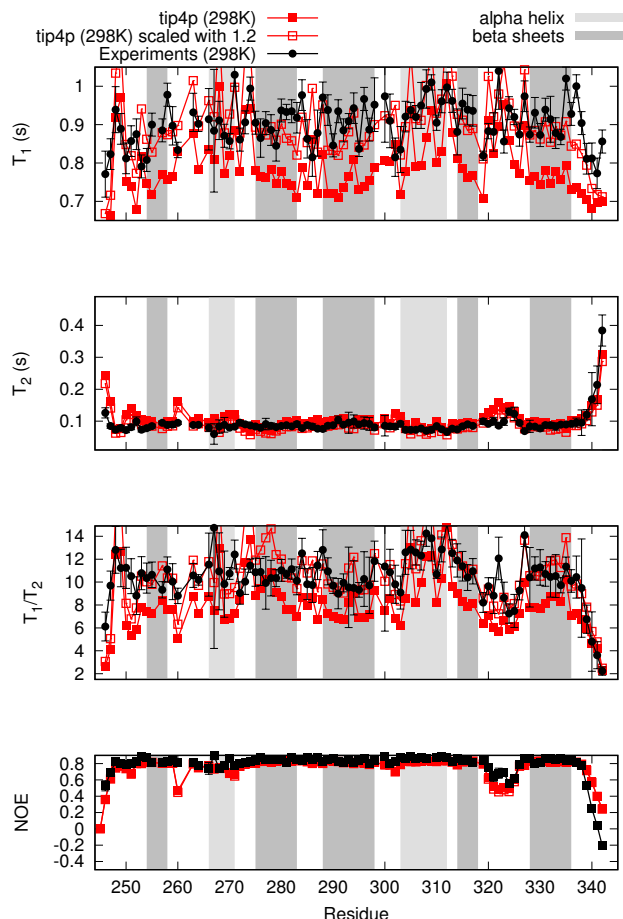


FIG. 5. Relaxation parameters for PsTonB from experiments and simulations with Amber-ildn and different water models. Overall rotational diffusion corrected with factor 1.2.

facts because deviation from experimental relaxation data is relatively large for these residues. Different orientations of alpha helix between residues 210-220 and decreased order parameters are not observed in contrast to PsTonB, except single large effective correlation time value at residue 218. The low resolution in NMR spectra [? ], however, suggest that the same phenomena is present but not observed in simulations, possibly due to timescale or force field issues.

#### IV. CONCLUSIONS

Rotation of protein inertia axes is observed to experience linear diffusion behaviour and overall diffusion component of rotational correlation functions of individual N-H bonds can be successfully fitted to the model assuming anisotropic diffusion for whole molecule.

Rotational diffusion of whole molecules is overestimated by a factor of  $\sim 3$  in simulations with tip3p water, in agreement with previous studies [? ]. The simulations with tip4p and opc4 water models give more realistic diffusion coefficients, which overestimate diffusion only with factors  $\sim 1$ -1.2.

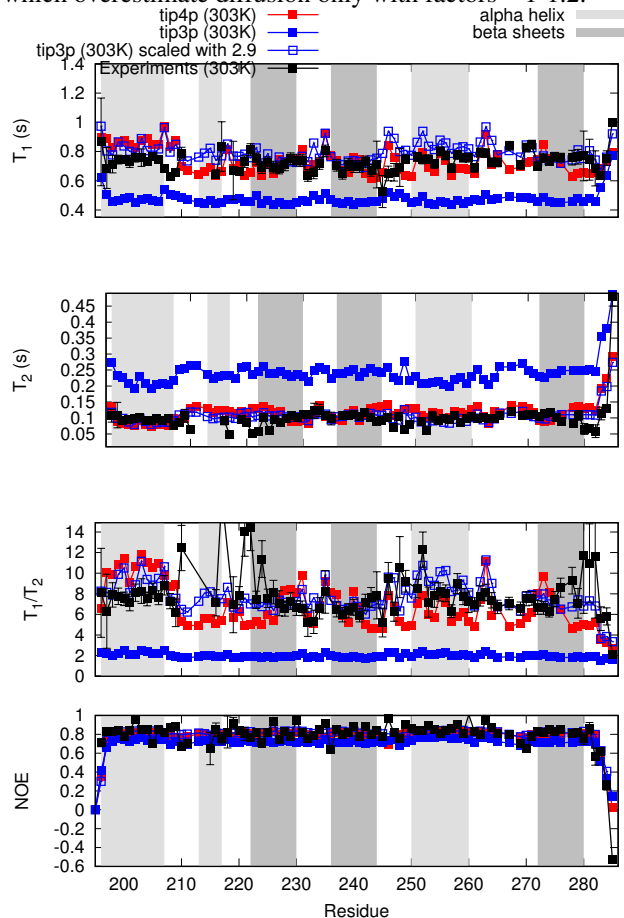


FIG. 6. Relaxation parameters for HpTonB short construct from experiments and simulations with Amber-ildn and different water models

The overestimated overall diffusion coefficient can be corrected post-simulationally to compare internal dynamics and order with experiments.

The presented methodology can be used to interpret spin relaxation experiments by using MD simulations [? ] and assess the quality of protein force fields against NMR experiments. The presented scaling of overall anisotropic diffusion allows this also for simulations with incorrect rotational diffusion due to water models, which is the case in simulations with tip3p.

#### ACKNOWLEDGMENTS

[1] A. Abragam, *The Principles of Nuclear Magnetism* (Oxford University Press, 1961).

[2] L. E. Kay, D. A. Torchia, and A. Bax, *Biochemistry* **28**, 8972



- (1989).
- [3]  $\tau_1 = (4D_{xx} + D_{yy} + D_{zz})^{-1}$ ,  $\tau_2 = (D_{xx} + 4D_{yy} + D_{zz})^{-1}$ ,  $\tau_3 = (D_{xx} + D_{yy} + 4D_{zz})^{-1}$ ,  $\tau_4 = [6(D + (D^2 - L^2)^{-1/2})^{-1}]^{-1}$ ,  $\tau_5 = [6(D - (D^2 - L^2)^{-1/2})^{-1}]^{-1}$ ,  $D = \frac{1}{3}(D_{xx} + D_{yy} + D_{zz})$  and  $L^2 = \frac{1}{3}(D_{xx}D_{yy} + D_{xx}D_{zz} + D_{yy}D_{zz})$ .
- [4] M. J. Abraham, T. Murtola, R. Schulz, S. Pll, J. C. Smith, B. Hess, and E. Lindahl, *SoftwareX* **12**, 19 (2015).
- [5] K. Lindorff-Larsen, S. Piana, K. Palmo, P. Maragakis, J. L. Klepeis, R. O. Dror, and D. E. Shaw, *Proteins: Structure, Function, and Bioinformatics* **78**, 1950 (2010).
- [6] W. L. Jorgensen, J. Chandrasekhar, J. D. Madura, R. W. Impey, and M. L. Klein, *J. Chem. Phys.* **79**, 926 (1983).
- [7] S. Izadi, R. Anandakrishnan, and A. V. Onufriev, *The Journal of Physical Chemistry Letters* **5**, 3863 (2014).
- [8] A. Ciragan, A. S. Aranko, I. Tascon, and H. Iwa, *Journal of Molecular Biology* **428**, 4573 (2016).
- [9] G. Bussi, D. Donadio, and M. Parrinello, *J. Chem. Phys.* **126** (2007).
- [10] M. Parrinello and A. Rahman, *J. Appl. Phys.* **52**, 7182 (1981).
- [11] T. Darden, D. York, and L. Pedersen, *J. Chem. Phys.* **98**, 10089 (1993).
- [12] U. L. Essman, M. L. Perera, M. L. Berkowitz, T. Larden, H. Lee, and L. G. Pedersen, *J. Chem. Phys.* **103**, 8577 (1995).
- [13] B. Hess, *J. Chem. Theory Comput.* **4**, 116 (2008).
- [14] M. Abraham, D. van der Spoel, E. Lindahl, B. Hess, and the GROMACS development team, *GROMACS user manual version 5.0.7* (2015).
- [15] R. T. McGibbon, K. A. Beauchamp, M. P. Harrigan, C. Klein, J. M. Swails, C. X. Hernández, C. R. Schwantes, L.-P. Wang, T. J. Lane, and V. S. Pande, *Biophysical Journal* **109**, 1528

(2015).

- [16] .
- [17] A. Nowacka, N. Bongartz, O. Ollila, T. Nylander, and D. Topgaard, *J. Magn. Res.* **230**, 165 (2013).
- [18] T. M. Ferreira, O. H. S. Ollila, R. Pigliapochi, A. P. Dabkowska, and D. Topgaard, *J. Chem. Phys.* **142**, 044905 (2015).

## SUPPLEMENTARY INFORMATION

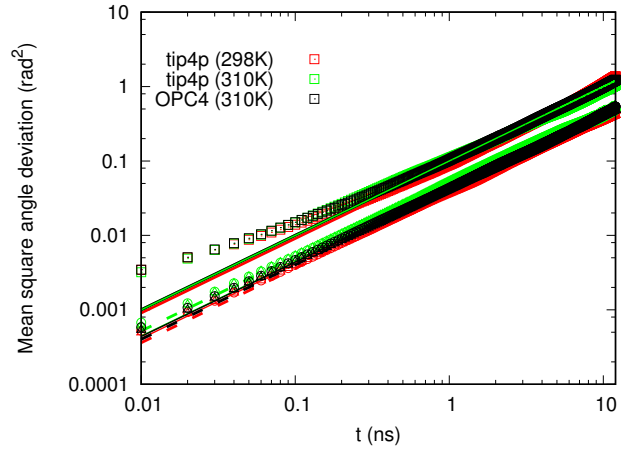


FIG. 7. The inertia tensor angles as a function of time and mean square angular deviations for PsTonB simulation with OPC water model.